TNFR2/14-3-3ε signaling complex instructs macrophage plasticity in inflammation and autoimmunity

Wenyu Fu, Wenhuo Hu, Young-Su Yi, Aubryanna Hettinghouse, Guodong Sun, Yufei Bi, Wenjun He, Lei zhang, Guanmin Gao, Jody Liu, Kazuhito Toyo-oka, Guozhi Xiao, David B. Solit, Png Loke, Chuan-ju Liu

This Supplementary Materials File Includes:

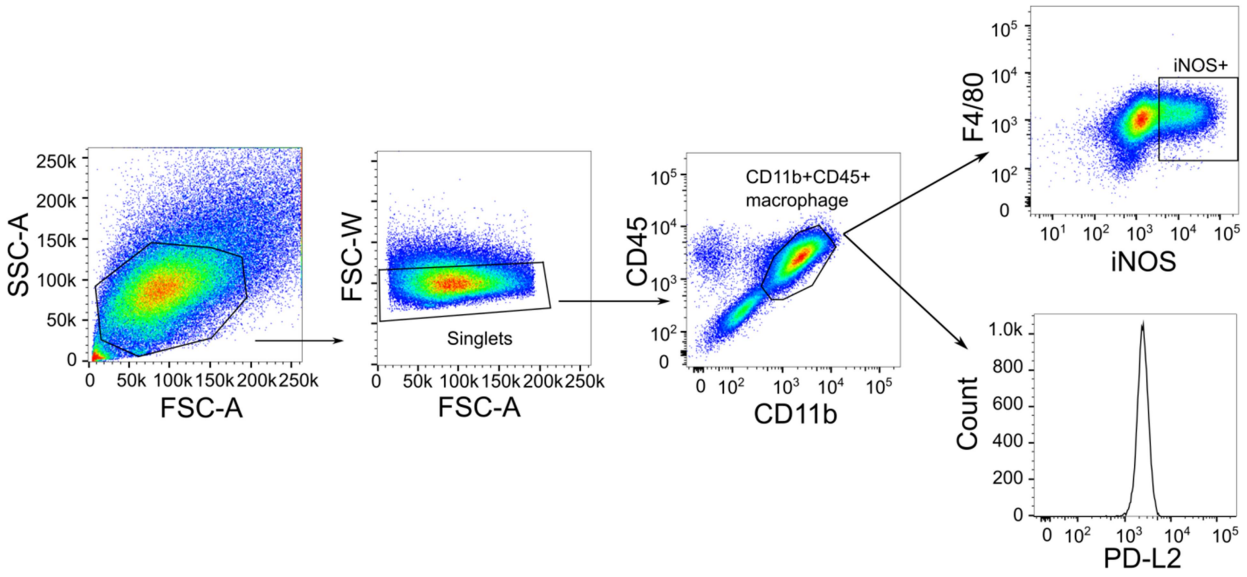

Supplementary Figure 1. Flow cytometry analysis of the expression of iNOS and PD-L2 on macrophages polarized to M1 or M2. Representative gating strategy is shown.

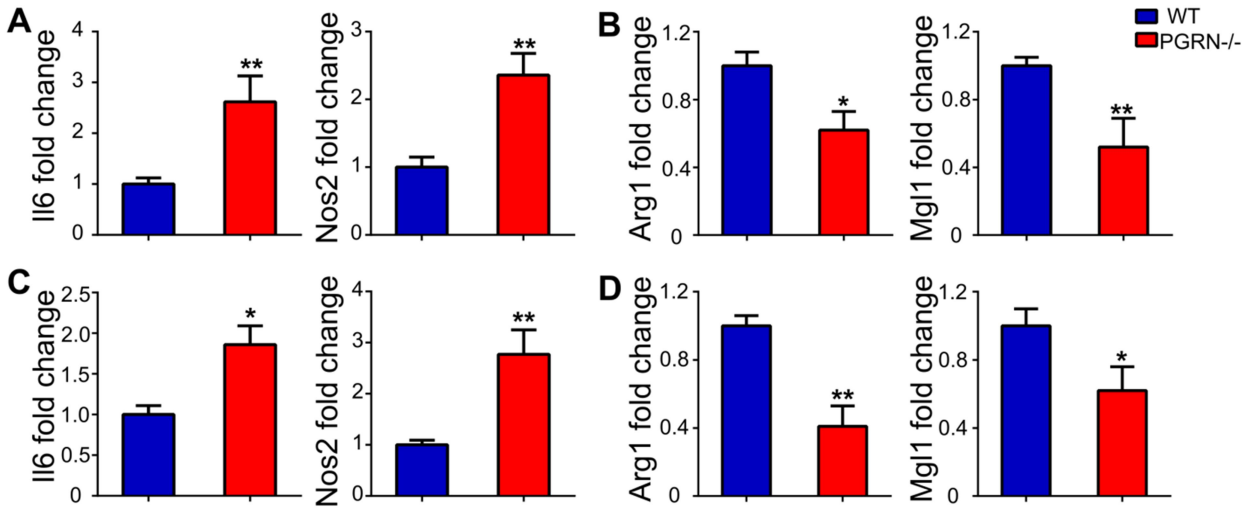

Supplementary Figure 2. Effects of PGRN deficiency on macrophage polarization and phenotypic switch. (A) Fold change of *Il6* and *Nos2* mRNA in WT and PGRN-/- BMDMs polarized to M1 with LPS/IFNγ for 18h. (B) Fold change of *Arg1* and *Mgl1* mRNA in WT and PGRN-/- BMDMs polarized to M2 with IL-4 for 18h. (C, D) BMDMs from WT and PGRN-/- were polarized to M2 (IL-4) or M1 (LPS and IFNγ) for 18 hours. Media were removed and M2 macrophages were treated with M1 stimuli (LPS and IFNγ) while M1 macrophages were treated with M2 stimuli (IL-4) for an additional 18h. qPCR was performed to measure the expression of *Nos2* and *Il6* in M2 macrophages polarized to M1 (C), and the expression of *Arg1* and *Mgl1* in M1 macrophages polarized to M2 (D). Data are mean ± SD; n = 3 biological replicates; * $P < 0.05$ or * * $P < 0.01$.

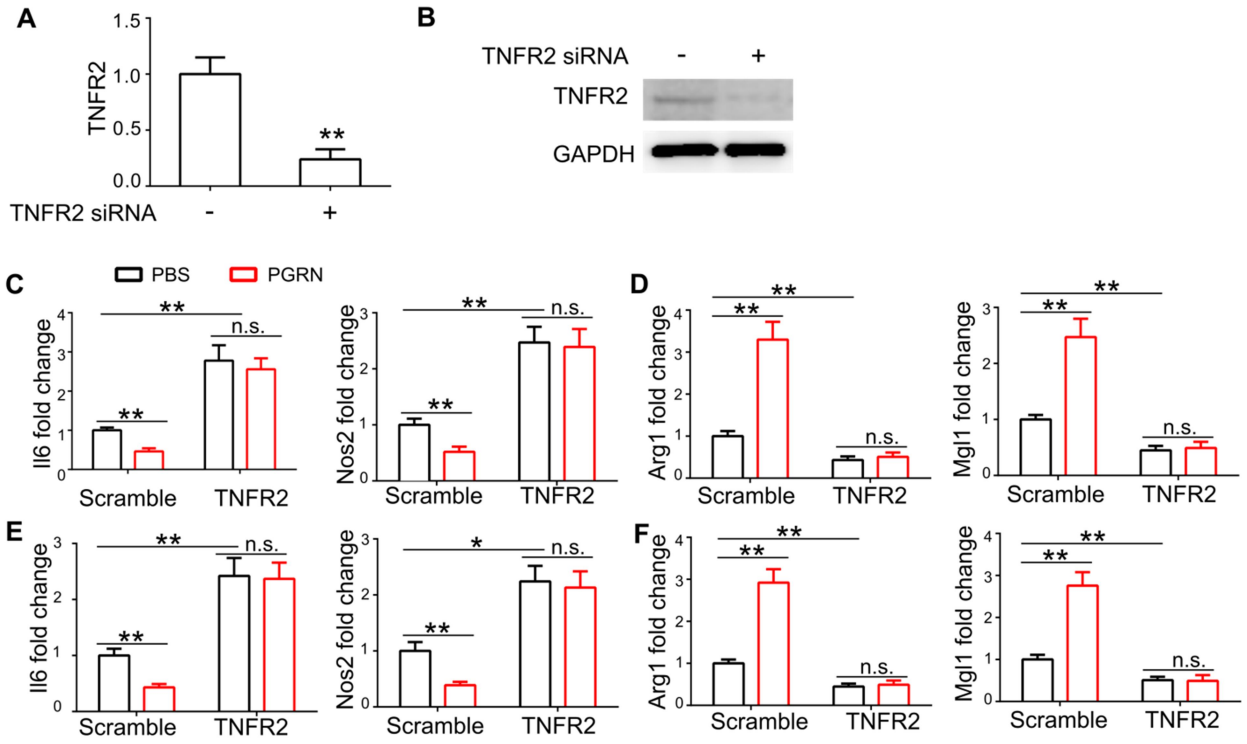

Supplementary Figure 3. Effects of TNFR2 knockdown and PGRN treatment on macrophage polarization and phenotypic switch in Raw264.7 macrophages. (A, B) Knockdown efficiency of TNFR2 in Raw264.7 macrophages measured by qRT-PCR (A) and Western blot (B). (C) Fold change of *Il6* and *Nos2* mRNA in control and TNFR2 knockdown Raw264.7 polarized to M1 with LPS/IFNγ in the presence or absence of PGRN for 18h. (D) Fold change of *Arg1* and *Mgl1* mRNA in control and TNFR2 knockdown Raw264.7 polarized to M2 with IL-4 in the presence or absence of PGRN for 18h. (E, F) Control and TNFR2 knockdown Raw264.7 were polarized to M2 (IL-4) or M1 (LPS and IFNγ) for 18 hours. Medium were removed, M2 macrophages were treated with M1 stimuli (LPS and IFNγ), and M1 macrophages were treated with M2 stimuli (IL-4) along with or without PGRN for an additional 18h. qPCR was performed to measure the expression of *Nos2* and *Il6* in M2 macrophages polarized to M1 (E), and the expression of *Arg1* and *Mgl1* in M1 macrophages polarized to M2 (F). C-F, data are mean ± SD; n = 3 biological replicates; Significant difference was analyzed by one-way ANOVA with post hoc Bonferroni test. * $P < 0.05$ or * * $P < 0.01$. "Scramble" and "TNFR2" indicate scramble siRNA and TNFR2 siRNA, respectively.

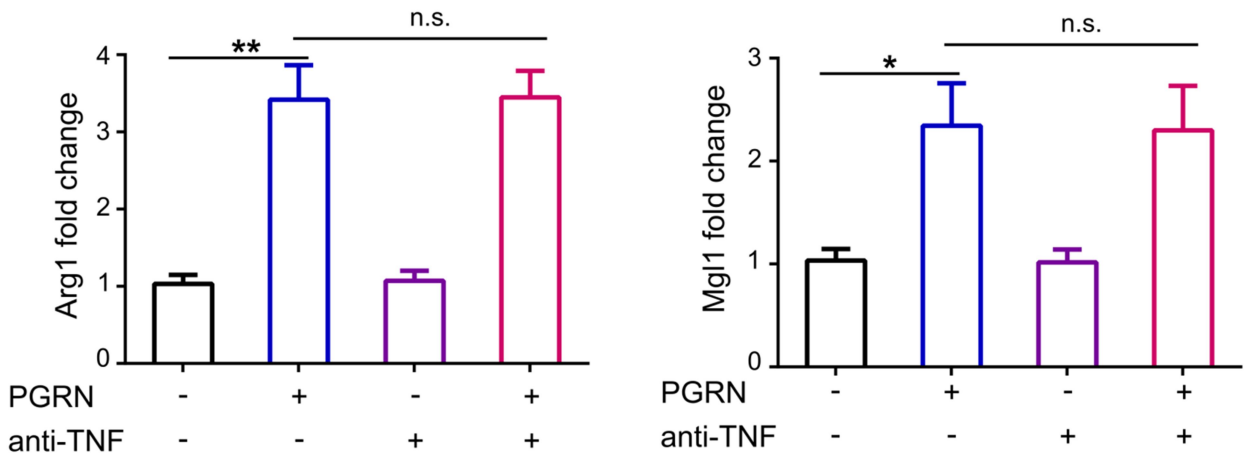

Supplementary Figure 4. Effects of blockade of TNFon IL-4 stimulated macrophage polarization. Fold change of *Arg1* and *Mgl1* mRNA in Raw264.7 macrophages polarized to M2 with IL-4 with or without 50ng/ml anti-TNF antibody (D2H4, Cell signaling Technology) and 200ng/ml PGRN for 18h. Significant difference was analyzed by one-way ANOVA with post hoc Bonferroni test. * $P < 0.05$ or * * $P < 0.01$.

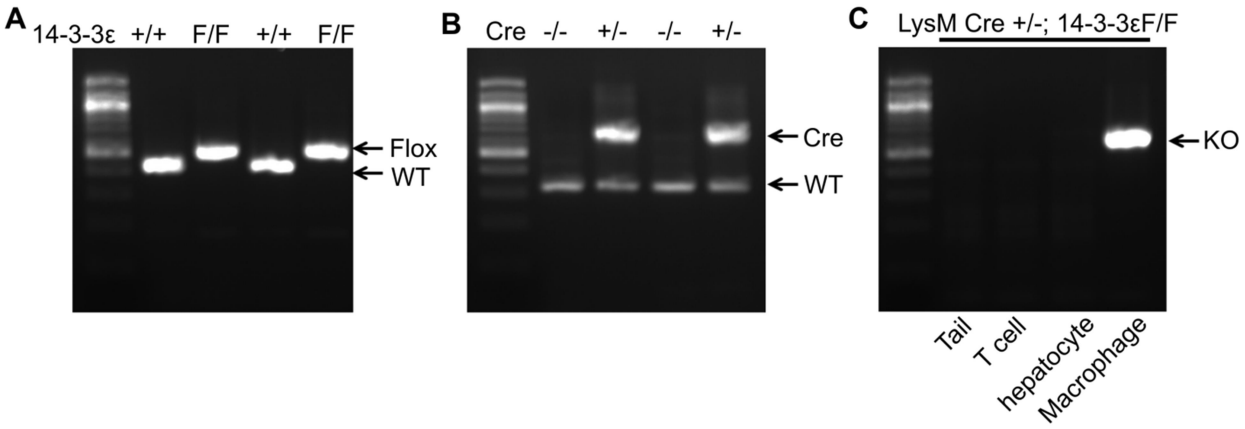

Supplementary Figure 5. Genotyping of the conditional 14-3-3ε knockout mice. Genomic DNA PCR detection of (A) 14-3-3ε floxed allele; (B) LysM Cre transgenic; and (C) 14-3-3ε knockout allele.

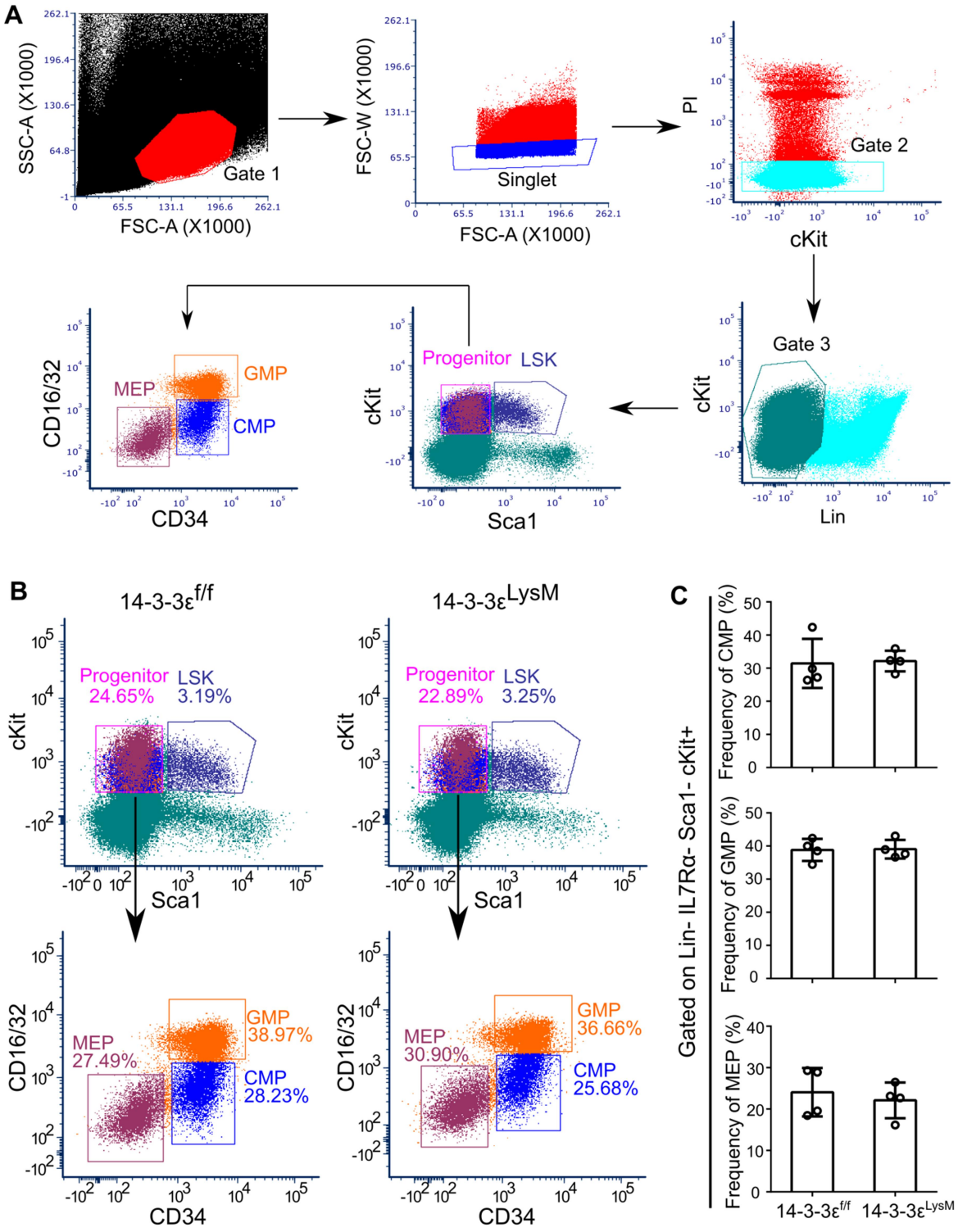

Supplementary Figure 6. Myeloid progenitors are not affected by *14-3-3ε* deficiency. (A) Flow cytometry gating strategy used to define CMPs (CD16/32^{low}CD34+), GMPs (CD16/32^{high} CD34+) and MEPs s (CD16/32^{low}CD34-) based on their CD16/32 and CD34 expression. (B) Representative flow cytometry plot for CMPs, GMPs and MEPs. (C) Frequency of CMPs, GMPs, and MEPs in bone marrow of 14-3-3ε and 14-3-3ε^{LysM} mice. n = 4 mice for each group.

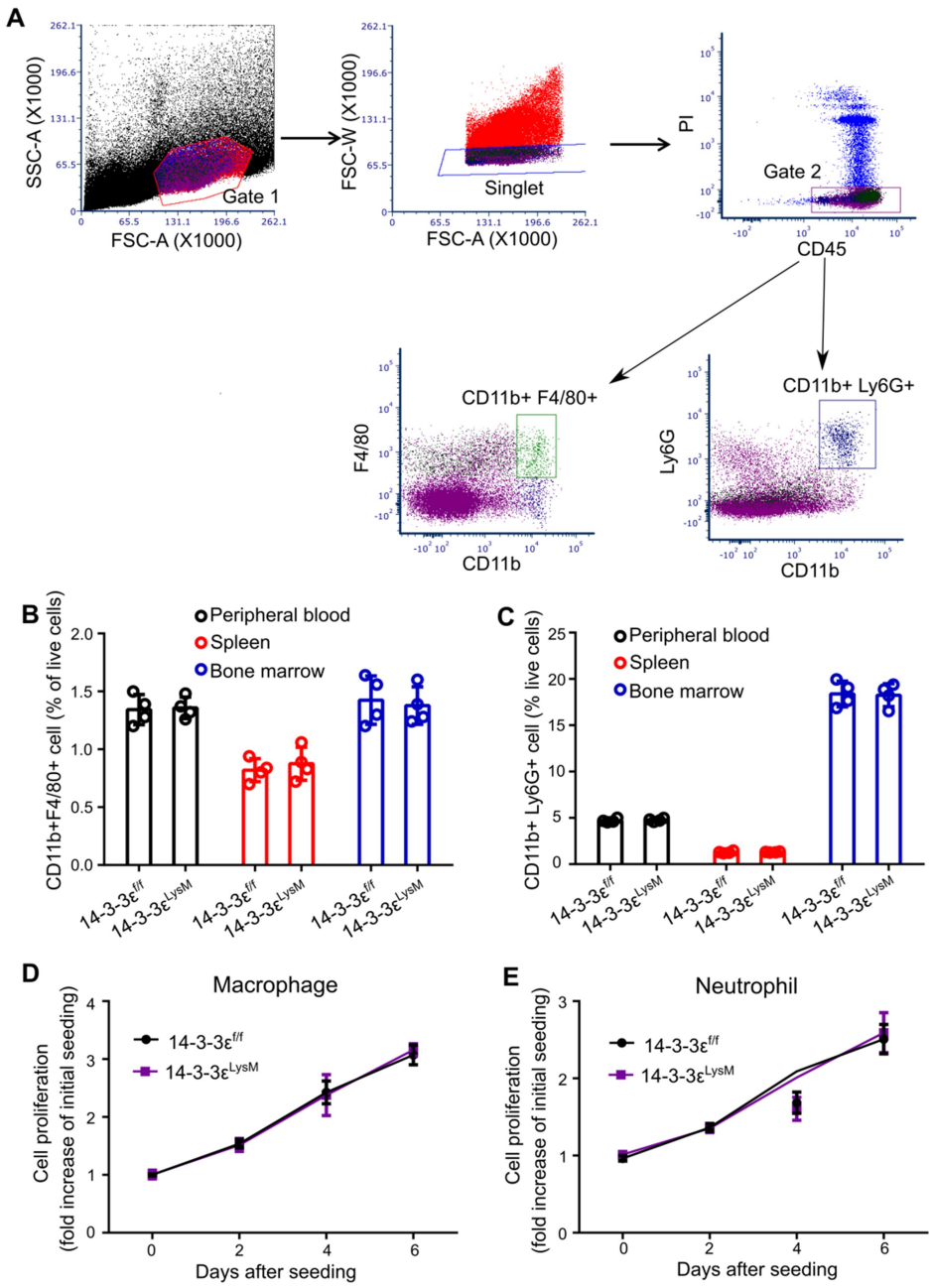

Supplementary Figure 7. Macrophage and neutrophil differentiation and proliferation are not dependent on 14-3-3ε. (A-C) Flow cytometry analysis of CD11b+F4/80+ monocyte/macrophage and CD11b+Ly6G+ neutrophil in peripheral blood, spleen and bone marrow from the indicated mice. Flow cytometry gating strategy used to define CD11b+F4/80+ monocyte/macrophage and neutrophil in spleen (A). Frequency of CD11b+F4/80+ (B) and CD11b+Ly6G+ cells (C) in peripheral blood, spleen and bone marrow from the indicated mice. n=4 mice for each group. (D, E) Proliferation of bone marrow derived macrophage (D) and neutrophil isolated from 14-3-3ε$^{f/f}$ and 14-3-3ε^{LysM} mice were measured by MTT assay. n = 4 mice for each group, data are mean ± SD.

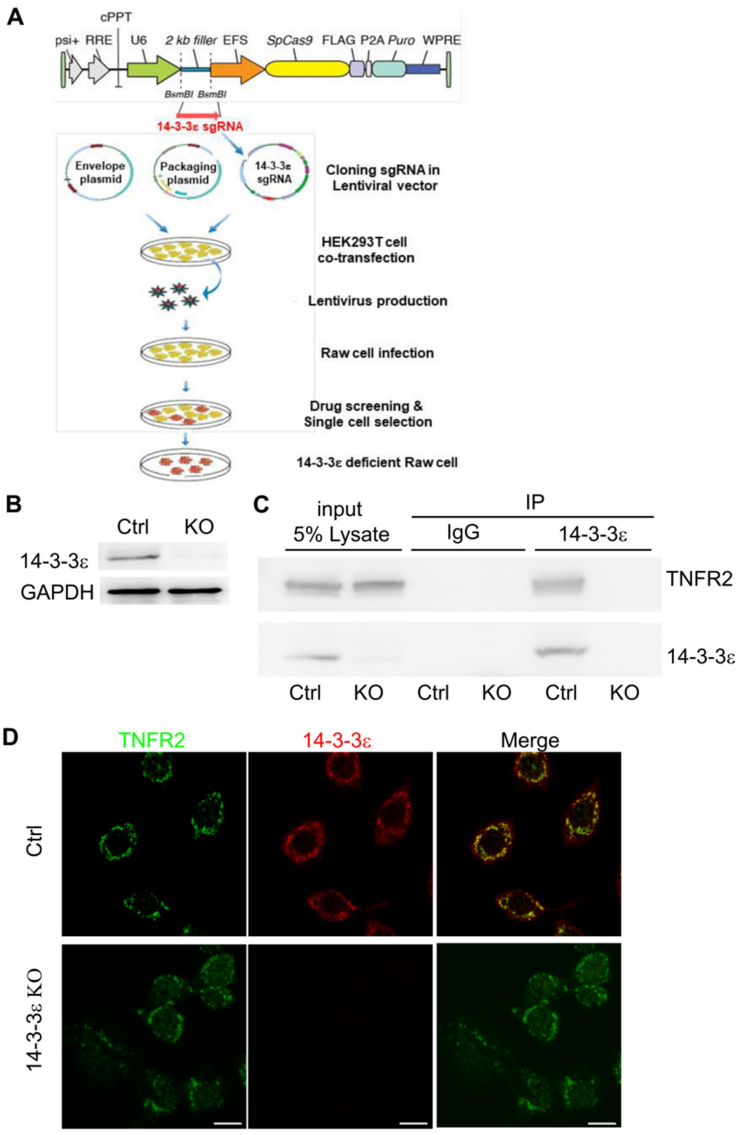

Supplementary Figure 8. 14-3-3ε is recruited to TNFR2 in Raw264.7 macrophages in response to PGRN treatment. (A) Schematic for generating 14-3-3ε-/- Raw264.7 cells using CRISPR/Cas9 technology. (B) Western blotting to confirm the loss of 14-3-3ε in 14-3-3ε-/- Raw264.7 cells. Cell lysates were examined by immunoblotting with 14-3-3ε antibody. (C) Control and 14-3-3ε-/- Raw264.7 macrophages were treated with 200ng/ml PGRN for 30min, then immunoprecipitated with 14-3-3ε antibody, and detection of TNFR2 and 14-3-3ε by immunoblotting. Results shown are representative of 3 biological replicates. (D) Immunofluorescence double staining of anti-TNFR2 and anti-14-3-3ε in Raw264.7 macrophages treated with 200ng/ml PGRN for 30min. Scale bar, 50μM.

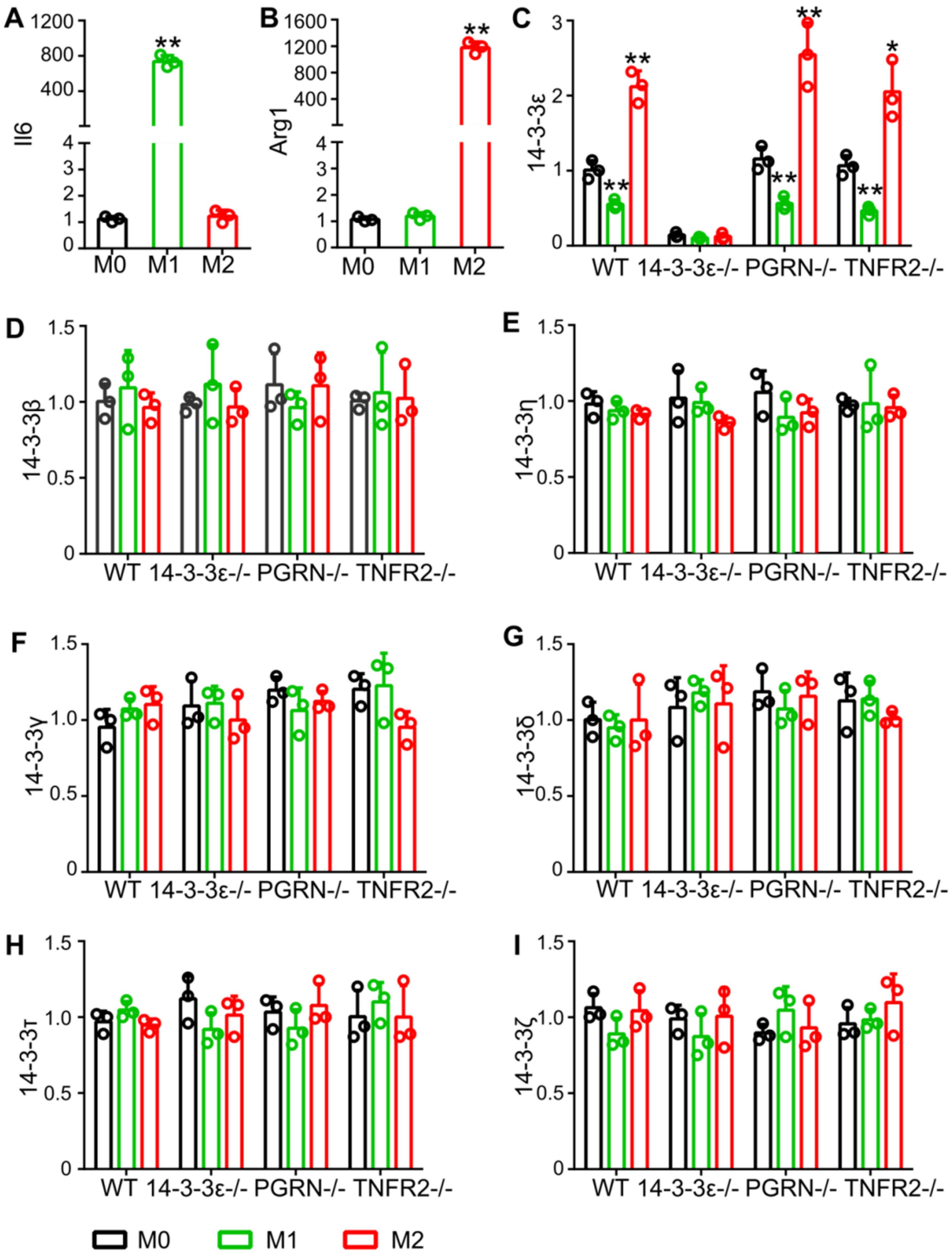

Supplementary Figure 9 *14-3-3ε* expression is differentially regulated in M1 and M2 macrophages. (A, B) Expression of *Il6* (A) and *Arg1* (B) after the induction of the M1 and M2 macrophages, respectively. (C-I) Expression of 14-3-3ε (C), β (D), η (E), γ (F), σ (G), τ (H), and ζ (I) in WT, 14-3-3ε-/-, PGRN-/-, and TNFR2-/- BMDMs polarized to M1 or M2 macrophages. Results are presented as relative to those of M0. Data are mean ± SD; n = 3 biological replicates; * $P < 0.05$ or * * $P < 0.01$.

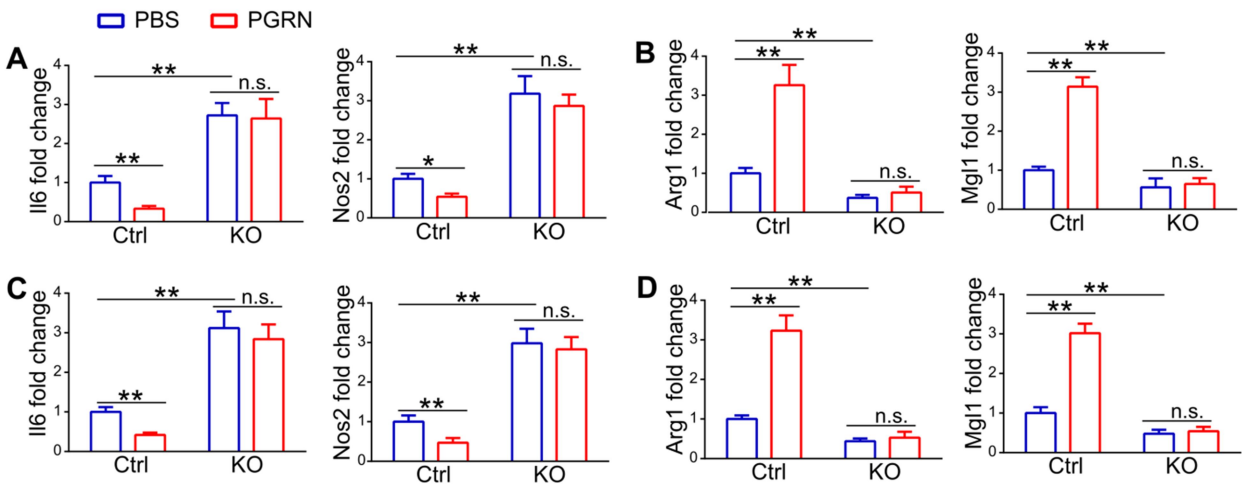

Supplementary Figure 10. Effects of 14-3-3ε deficiency and PGRN treatment on macrophage polarization and phenotypic switch in Raw264.7 macrophages. (A) Fold change of *Il6* and *Nos2* mRNA in control and 14-3-3ε KO Raw264.7 polarized to M1 with LPS/IFNγ in the presence or absence of PGRN for 18h. (B) Fold change of *Arg1* and *Mgl1* mRNA in control and 14-3-3ε KO Raw264.7 polarized to M2 with IL-4 in the presence or absence of PGRN for 18h. (C, D) Control and 14-3-3ε KO Raw264.7 were polarized to M2 (IL-4) or M1 (LPS and IFNγ) for 18 hours. Medium were removed, M2 macrophages were treated with M1 stimuli (LPS and IFNγ), and M1 macrophages were treated with M2 stimuli (IL-4) along with or without PGRN for an additional 18h. qPCR was performed to measure the expression of *Nos2* and *Il6* in M2 macrophages polarized to M1 (C), and the expression of *Arg1* and *Mgl1* in M1 macrophages polarized to M2 (D). Data are mean ± SD; n = 3 biological replicates; Significant difference was analyzed by one-way ANOVA with post hoc Bonferroni test. * $P < 0.05$ or * * $P < 0.01$.

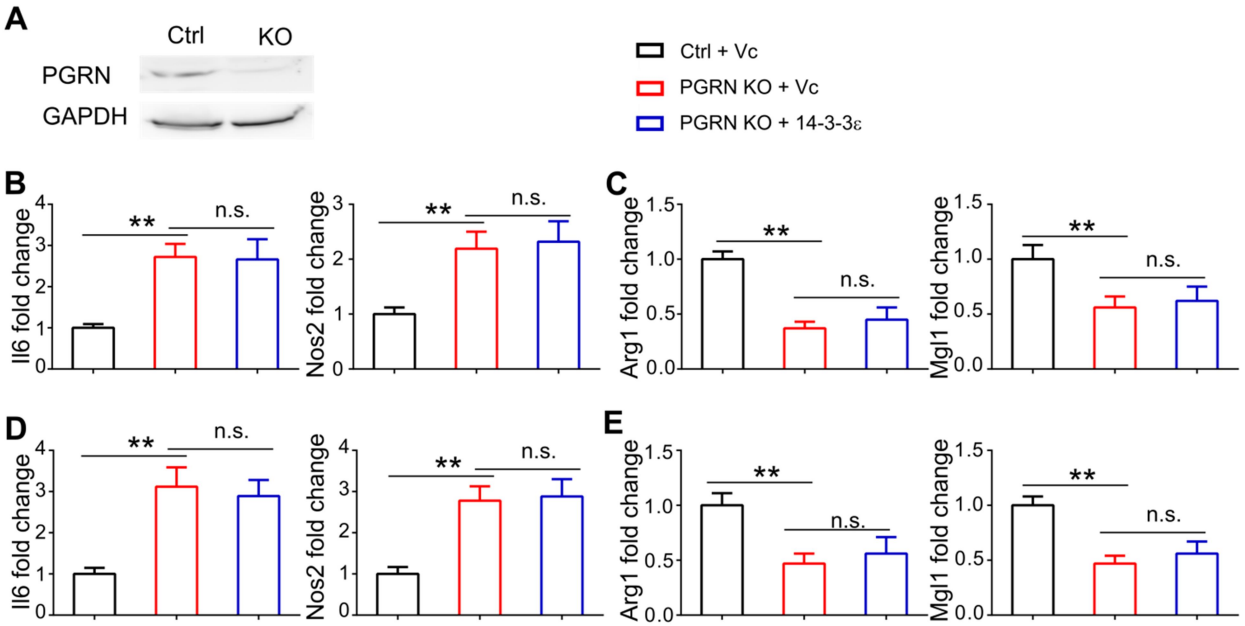

Supplementary Figure 11. Over-expression of 14-3-3ε in PGRN KO macrophages fails to rescue PRGN's effects on macrophage polarization and phenotypic switch. (A) Generation of PGRN KO Raw264.7 macrophages using Crispr-Cas9 technique. Western blot was used to validate the knockout efficiency of PGRN. (B) Fold change of *Il6* and *Nos2* mRNA in control and PGRN KO Raw264.7 polarized to M1 with LPS/IFNγ for 18h following re-expression of 14-3-3ε. (C) Fold change of *Arg1* and *Mgl1* mRNA in control and PGRN KO Raw264.7 polarized to M2 with IL-4 for 18h following re-expression of 14-3-3ε. (D, E) Re-expression of 14-3-3ε in PGRN KO Raw264.7 cells followed by polarizing to M2 (IL-4) or M1 (LPS and IFNγ) for 18 hours. Medium were removed and then M2 macrophages were treated with M1 stimuli (LPS and IFNγ); M1 macrophages were treated with M2 stimuli (IL-4) along with or without PGRN for an additional 18h. qPCR was performed to measure the expression of *Nos2* and *Il6* in M2 macrophages polarized to M1 (D), and the expression of *Arg1* and *Mgl1* in M1 macrophages polarized to M2 (E). B-E, data are mean ± SD; n = 3 biological replicates; Significant difference was analyzed by one-way ANOVA with post hoc Bonferroni test. * $P < 0.05$ or * * $P < 0.01$. Vc, empty vector; 14-3-3ε, pCMV-Flag-14-3-3ε plasmid.

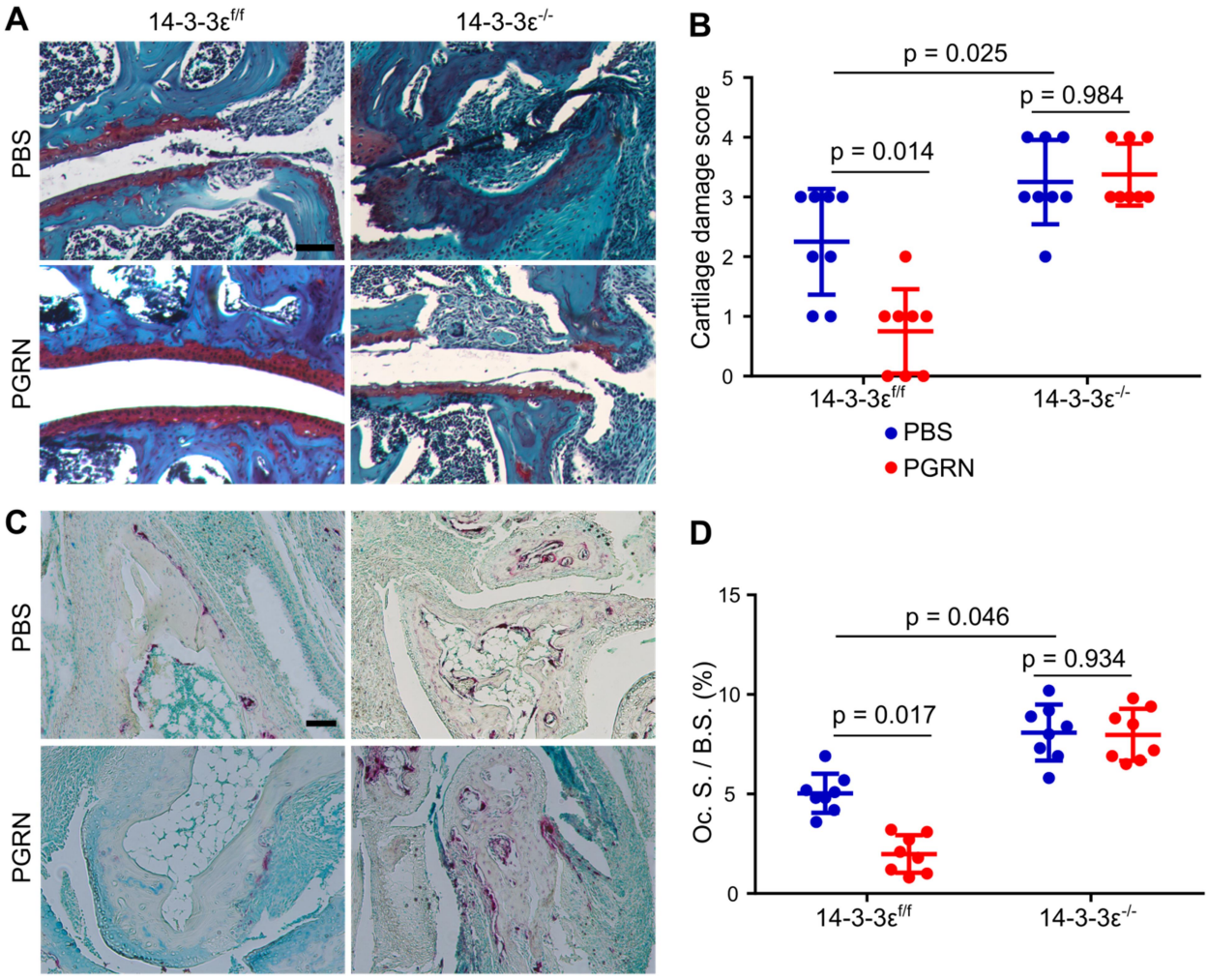

Supplementary Figure 12 Effects of global 14-3-3ε deletion on the progression of collagen-induced arthritis. (A) Representative image of Safranin O staining of the ankle joints from each experimental group. (B) Quantitative analysis of cartilage damage in each group. (C) Representative image of TRAP staining of the ankle joints from each experimental group. (D) Quantitative analysis of osteoclast surface per bone surface (Oc. S./ B.S.). Scale bar, 100 μM. Data are mean ± SD; n = 8 mice per group. Significant difference was analyzed by one-way ANOVA with post hoc Bonferroni test.

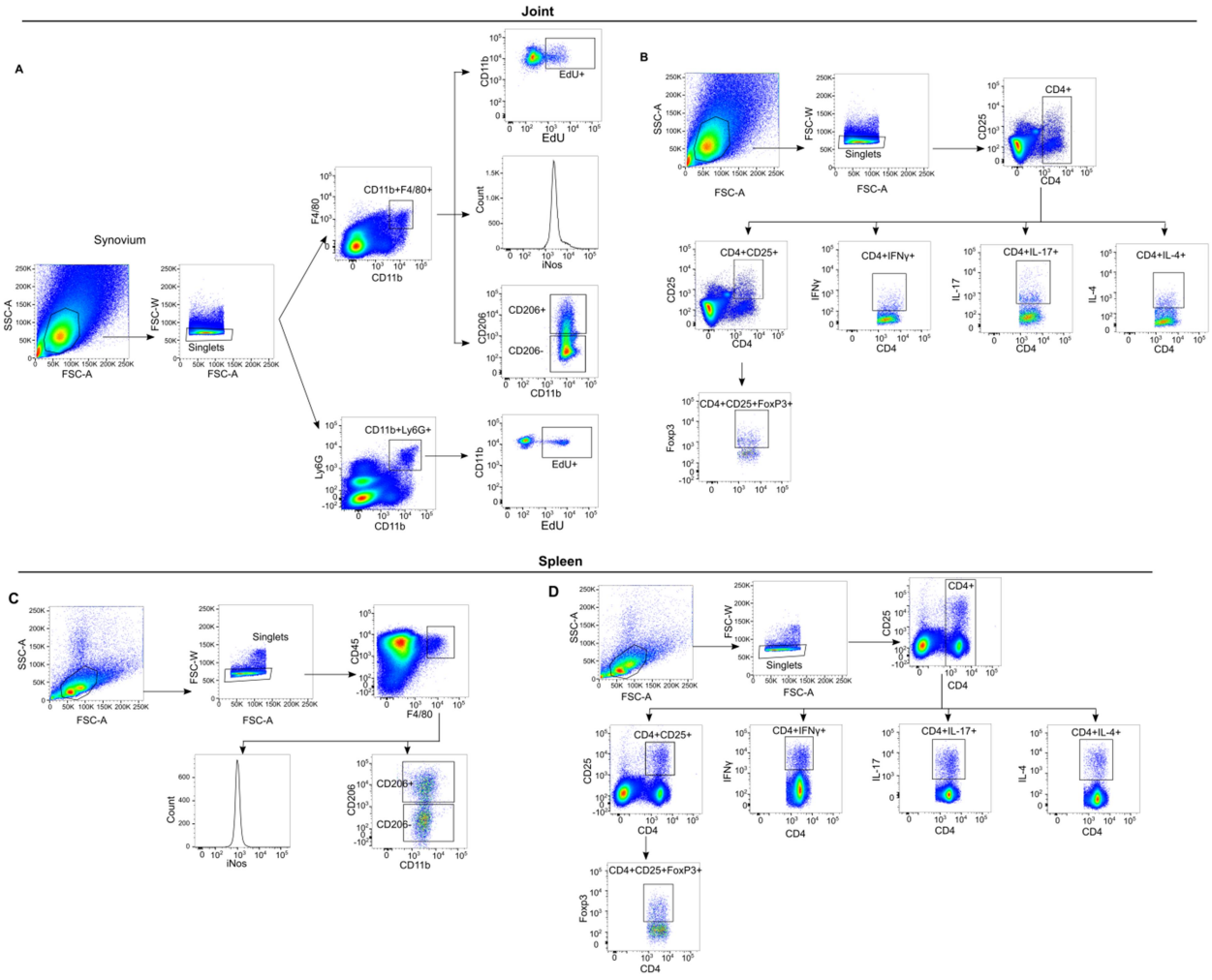

Supplementary Figure 13. Flow cytometry gating strategy used to define immune cells in joint and spleen isolated from CIA mice. (A, C) Outline of gating strategy for CD11b+F4/80+, EdU+CD11b+F4/80+, iNos and CD206+ in CD11b+F4/80+ cells, CD11b+Ly6G+ and EdU+CD11b+Ly6G+ cells in joint (A) and spleen (C). (B, D) Outline of gating strategy for Treg, Th1, Th17 and Th2 cells in joint (B) and spleen (D).

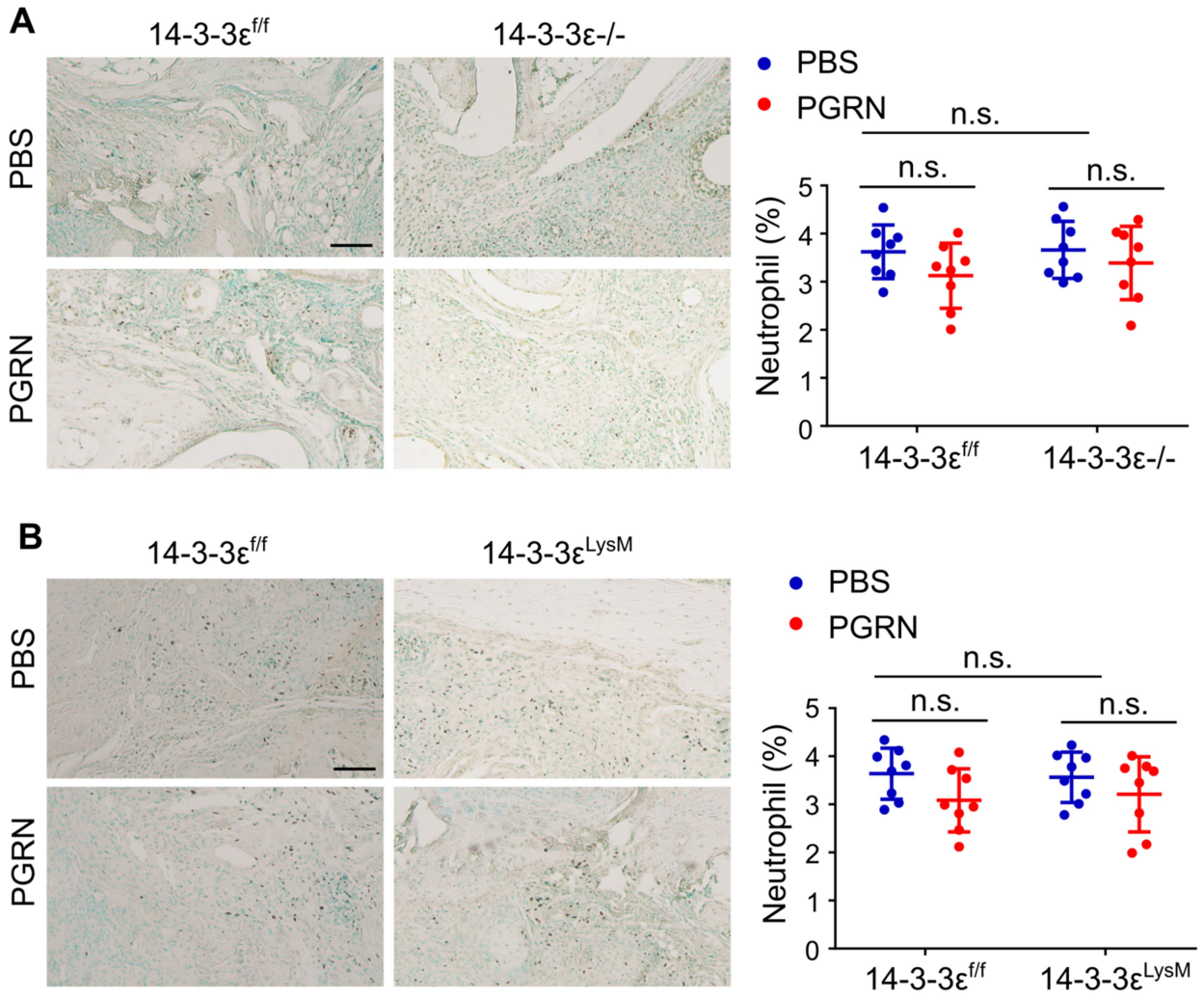

Supplementary Figure 14. Genetic 14-3-3ε deficiency does not affect activated neutrophil in the arthritic joints. Immunohistochemistry staining and quantification of activated neutrophil marker myeloperoxidase in joint sections of 14-3-3ε$^{f/f}$, 14-3-3ε-/- (A) and 14-3-3ε$^{f/f}$, 14-3-3ε^{LysM} (B) mice with CIA. n=8 mice for each group; significant difference was analyzed by one-way ANOVA with post hoc Bonferroni test, scale bar 100μM.

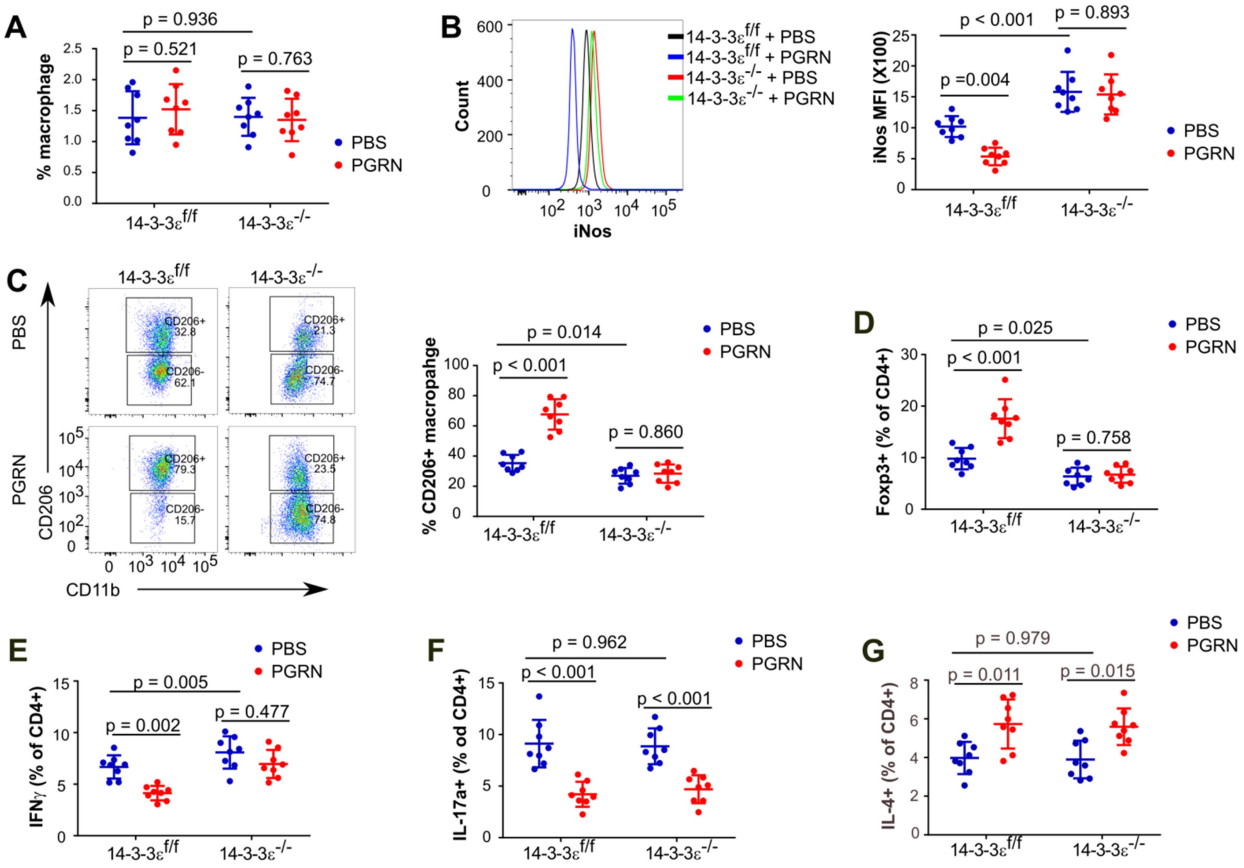

Supplementary Figure 15. The effects of global 14-3-3ε deletion on macrophages and CD4+ T cell subtypes in spleen of the mice with CIA. Flow cytometry analyses of percentage of total macrophages (CD11b+F4/80+) (A), iNos MFI of the macrophages (B), percentage of CD206+ macrophages in total macrophages (C), and percentage of Treg (D), Th1 (E), Th17 (F), and Th2 (G) cells in CD4+ T cells in spleen harvested from indicated mice with CIA. Data are mean ± SD; n = 8 mice per group; significant difference was analyzed by one-way ANOVA with post hoc Bonferroni test.

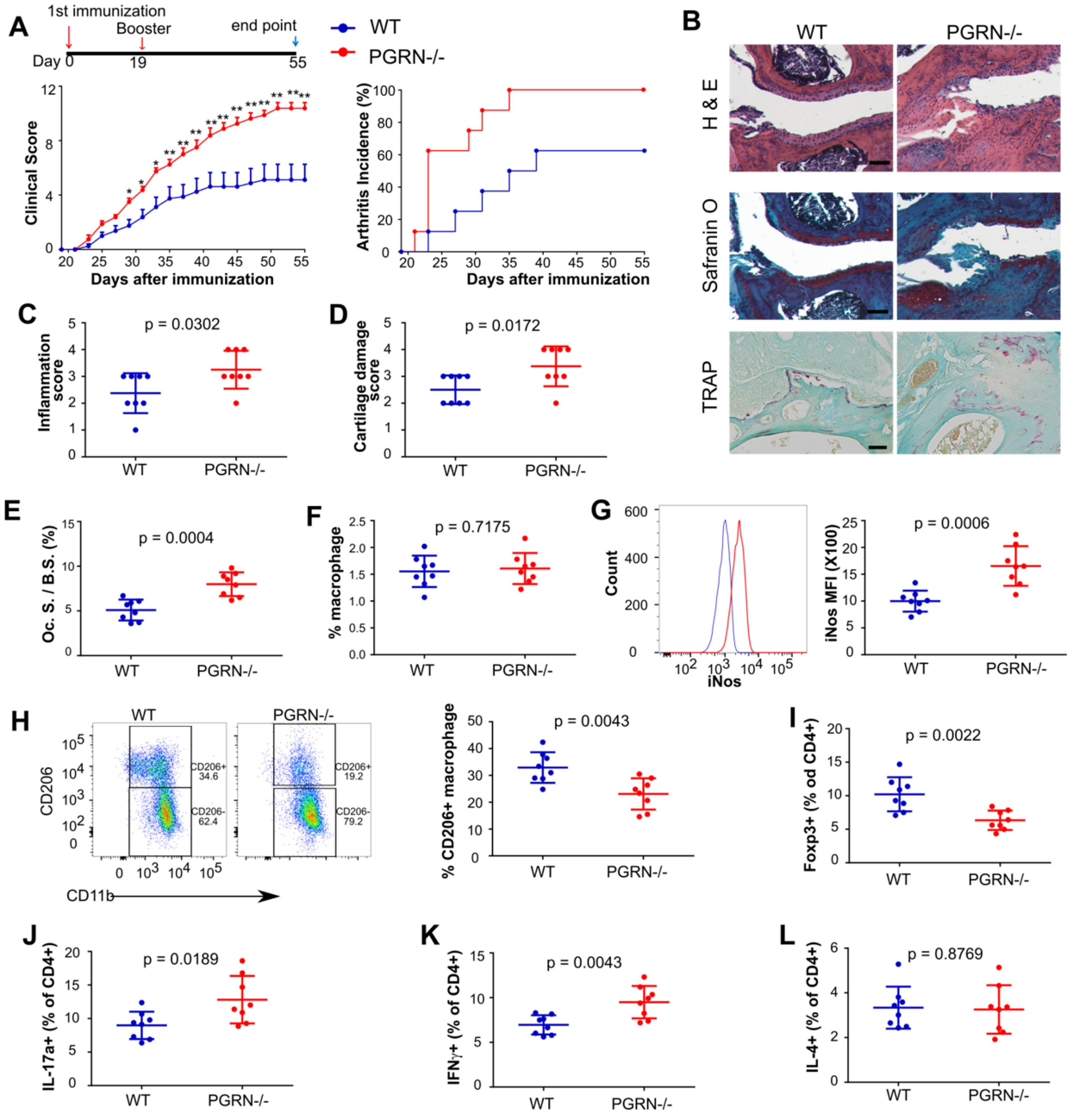

Supplementary Figure 16. PGRN deficiency enhances inflammation in mice with collagen induced arthritis. (A) Clinical arthritis scores and incidence of arthritis in the indicated mice with CIA. Data are mean ± SEM; n = 8 mice per group; * $P < 0.05$ or ** $P < 0.01$. (B-E) Representative images of H&E, Safranin O and TRAP staining (B), and quantification of histomorphometric analysis of synovial inflammation (C), cartilage damage (D), and Oc. S./B.S. (E) of ankle joints. Scale bar, 100 μM. (F-L) Flow cytometry analyses of percentage of macrophages (F), iNos MFI of macrophages (G), percentage of CD206+ macrophages in total macrophages (H), and percentage of Treg (I), Th17 (J), Th1 (K), and Th2 (L) cells in CD4+ T cells in spleen harvested from indicated mice with CIA.C-L, data are mean ± SD; n = 8 mice per group, significant difference was analyzed by unpaired t-test.

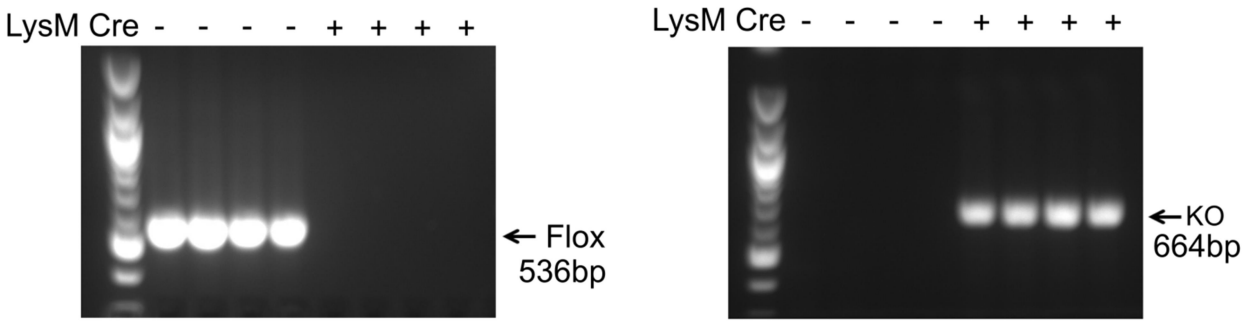

Supplementary Figure 17. Efficient deletion of 14-3-3ε in macrophages presented in the joints of 14-3-3ε^{LysM} mice with CIA. Macrophages were isolated from the joints of 14-3-3ε$^{f/f}$ and 14-3-3ε^{LysM} mice with CIA, and the deletion efficiency of 14-3-3ε in these cells were analyzed by PCR. n = 4 mice for each group.

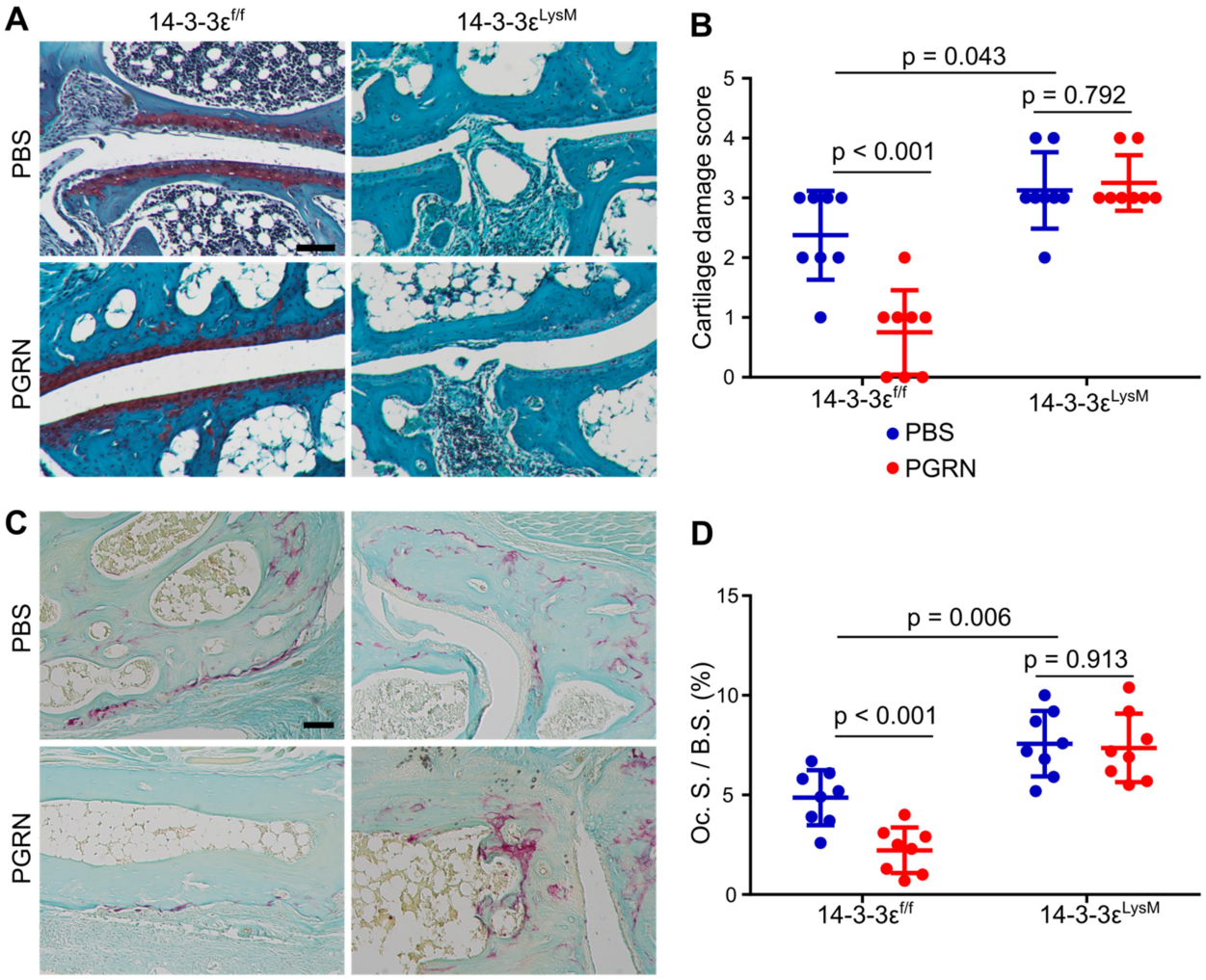

Supplementary Figure 18. Effects of myeloid specific 14-3-3ε deletion on the progression of collagen-induced arthritis. (A) Representative image of Safranin O staining of the ankle joints from each experimental group. (B) Quantitative analysis of cartilage damage in each group. (C) Representative image of TRAP staining of the ankle joints from each experimental group. (D) Quantitative analysis of osteoclast surface per bone surface (Oc. S./ B.S.). Scale bar, 100 μM. Data are mean ± SD; n = 8 mice per group. Significant difference was analyzed by one-way ANOVA with post hoc Bonferroni test.

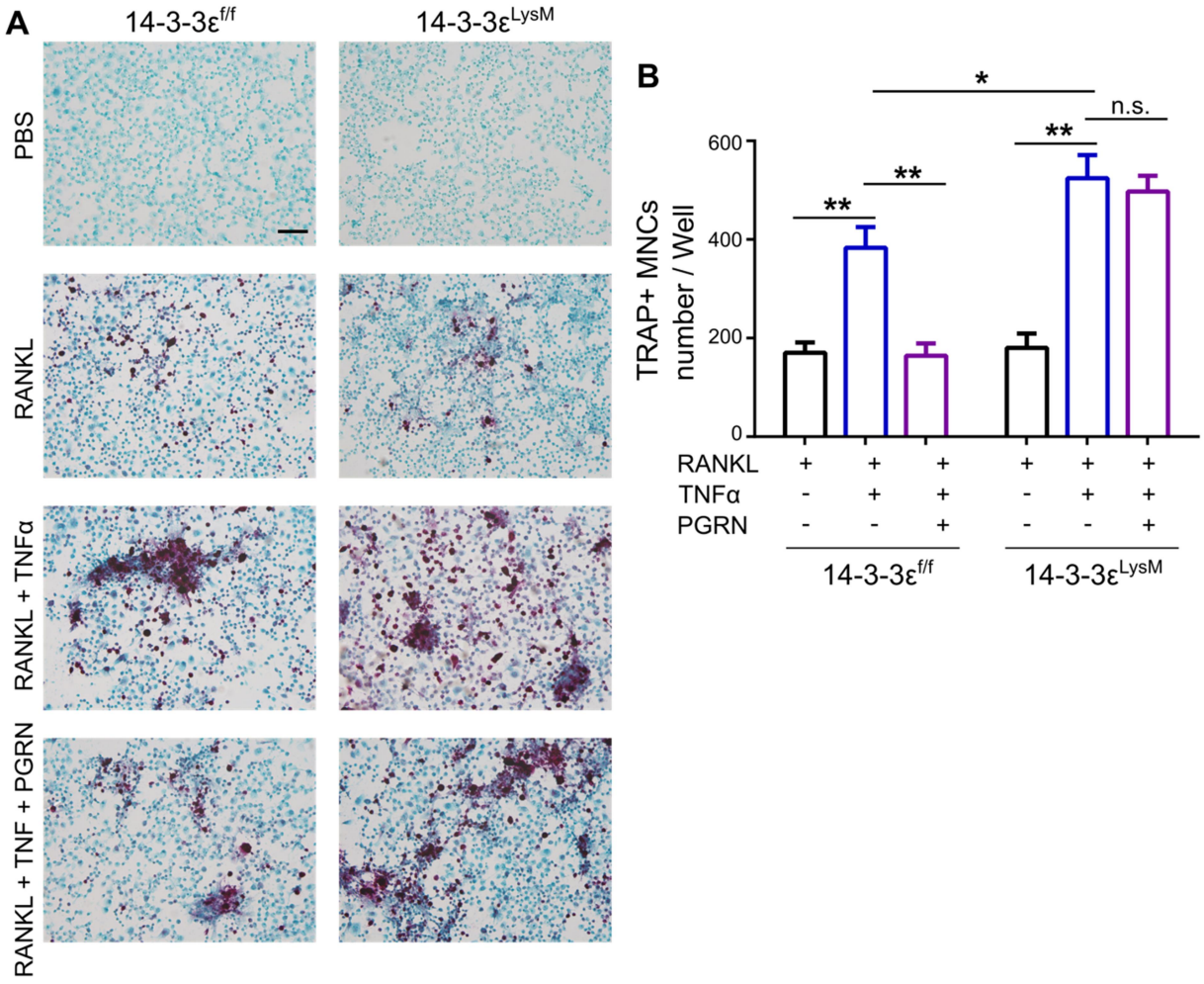

Supplementary Figure 19. 14-3-3ε was involved in PGRN's inhibition of TNFα enhanced osteoclastogenesis. (A) BMDMs isolated from 14-3-3εf/f and 14-3-3εLysM mice were cultured with 10ng/ml M-CSF for 3days, before differentiated to osteoclasts with 10ng/ml M-CSF, 50ng/ml RANKL, 10ng/ml TNFα, or combinations, as indicated, with or without 200ng/ml PGRN for 5 days before TRAP staining. Scale bar, 100 μm. (B) Quantified number of TRAP+ multinucleated cells/well as shown in (A). n = 4 biological replicates; Data are mean ± SD, significant difference was analyzed by one-way ANOVA with post hoc Bonferroni test; **P* < 0.05; ***P* < 0.01.

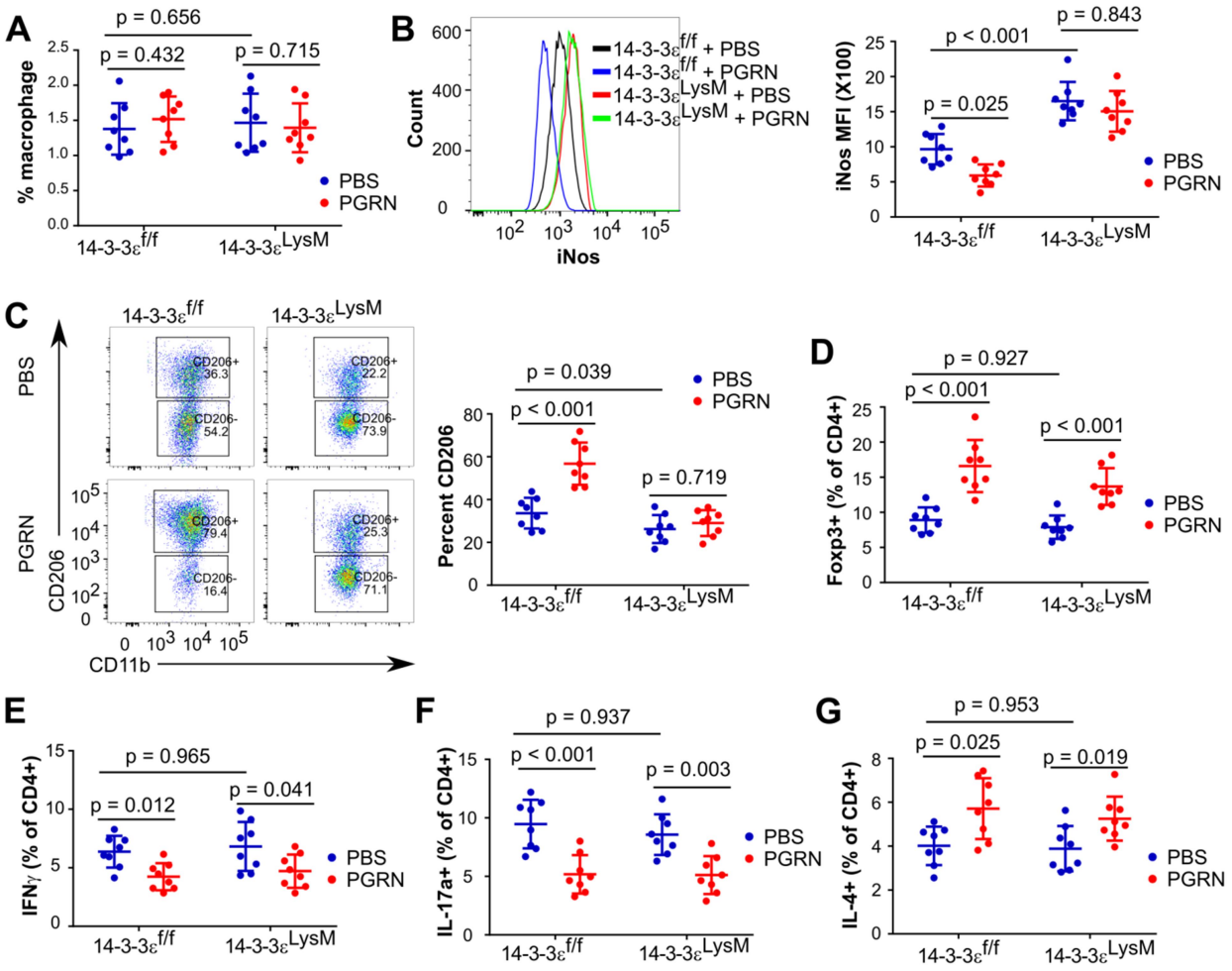

Supplementary Figure 20. The effects of myeloid specific 14-3-3ε deletion on macrophages and CD4+ T cell subtypes in spleens of the mice with CIA. Flow cytometry analyses of percentage of macrophages (CD11b+F4/80+) (A), iNos MFI of macrophages (B), percentage of CD206+ macrophages in total macrophages (C), and percentage of Treg (D), Th1 (E), Th17 (F), and Th2 (G) cells in CD4+ T cells in spleens harvested from the mice with CIA, as indicated. Data are mean ± SD; n = 8 mice per group; significant difference was analyzed by one-way ANOVA with post hoc Bonferroni test.

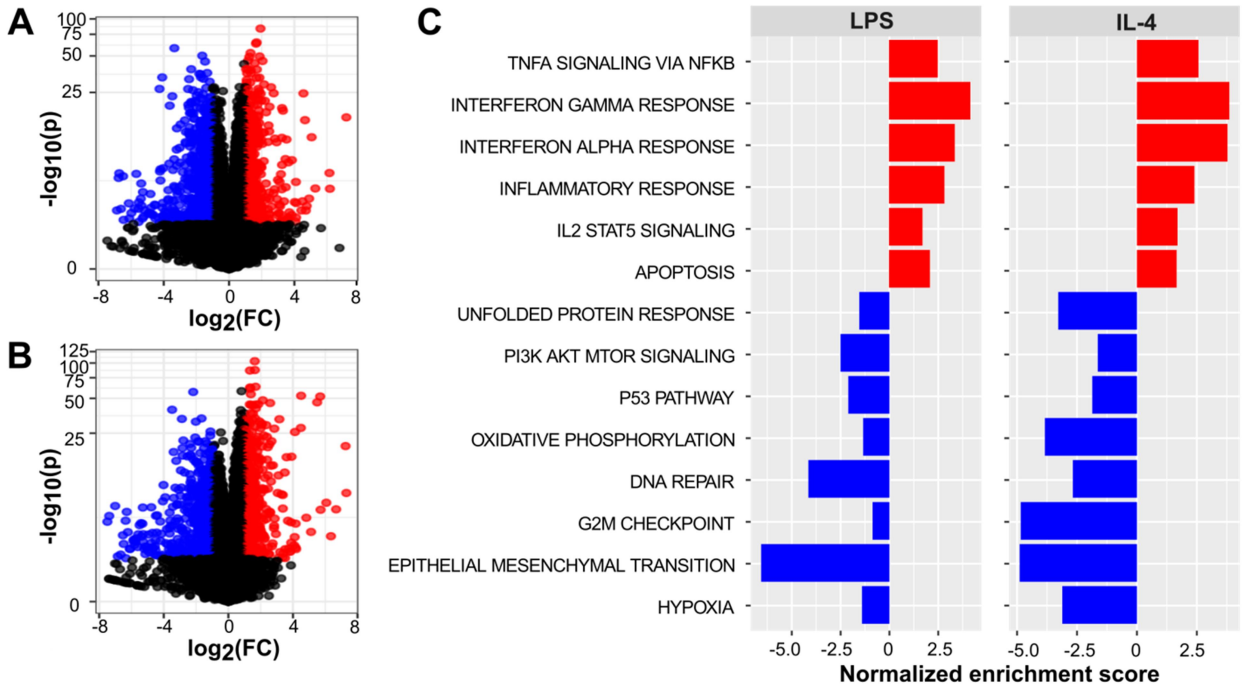

Supplementary Figure 21. PGRN deficient macrophages show an altered transcriptome signature. (A, B) Volcano plots of differentially expressed transcripts in LPS/IFN-γ (A) or IL-4 (B) polarized WT and PGRN-/- macrophages obtained by RNA sequencing. n = 3 biological replicates. Linear models with empirical Bayes statistic (Limma) were used for differential expression. Genes in red or blue are up-regulated or down-regulated, respectively, in PGRN-/- as compared to WT with Benjamini–Hochberg adjusted $P < 0.05$. (C) Gene Set Enrichment Analysis (GSEA) analysis using hallmark gene sets from the Molecular Signature Database. The statistically significant signatures were filtered by gene sets with false discovery rates (FDR) < 0.25. Red bars represented the pathways up-regulated in the PGRN-/- macrophages and blue bars indicated those enriched in WT macrophages.

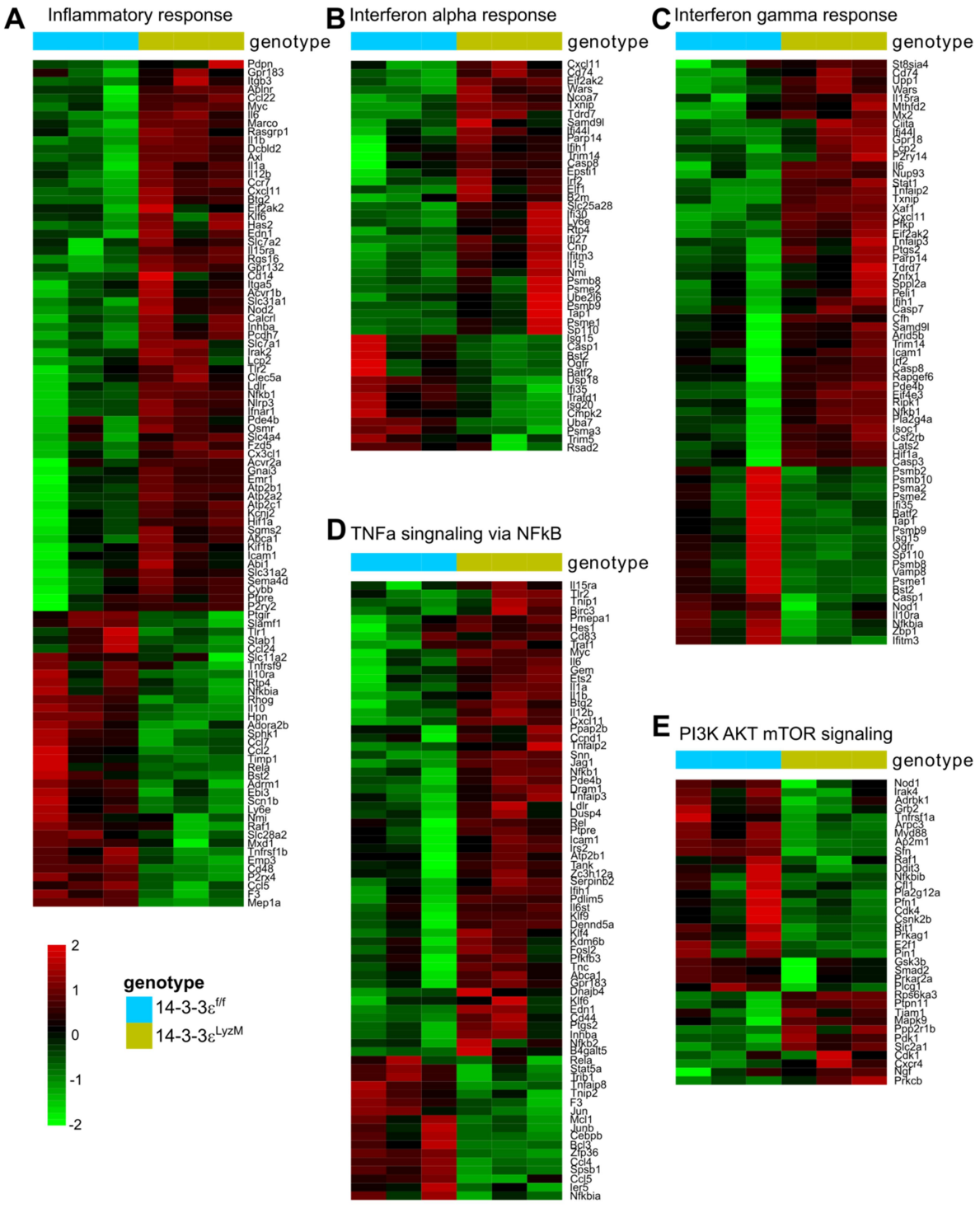

Supplementary Figure 22. Effect of 14-3-3ε deficiency on M1 macrophage mRNA expression *in vitro*. (A-E) Heat map with GSEA normalized enrichment scores of gene expression profile of 14-3-3$\varepsilon^{f/f}$ and 14-3-3ε^{LysM} BMDMS polarized to M1 obtained by RNA sequencing of interferon gamma (A), interferon alpha (B), inflammatory response (C), TNFα signaling via NF-κB (D) and PI3K AKT mTOR signaling (E) pathways, gene sets from Hallmark. Data are from n = 3 biologically independent samples.

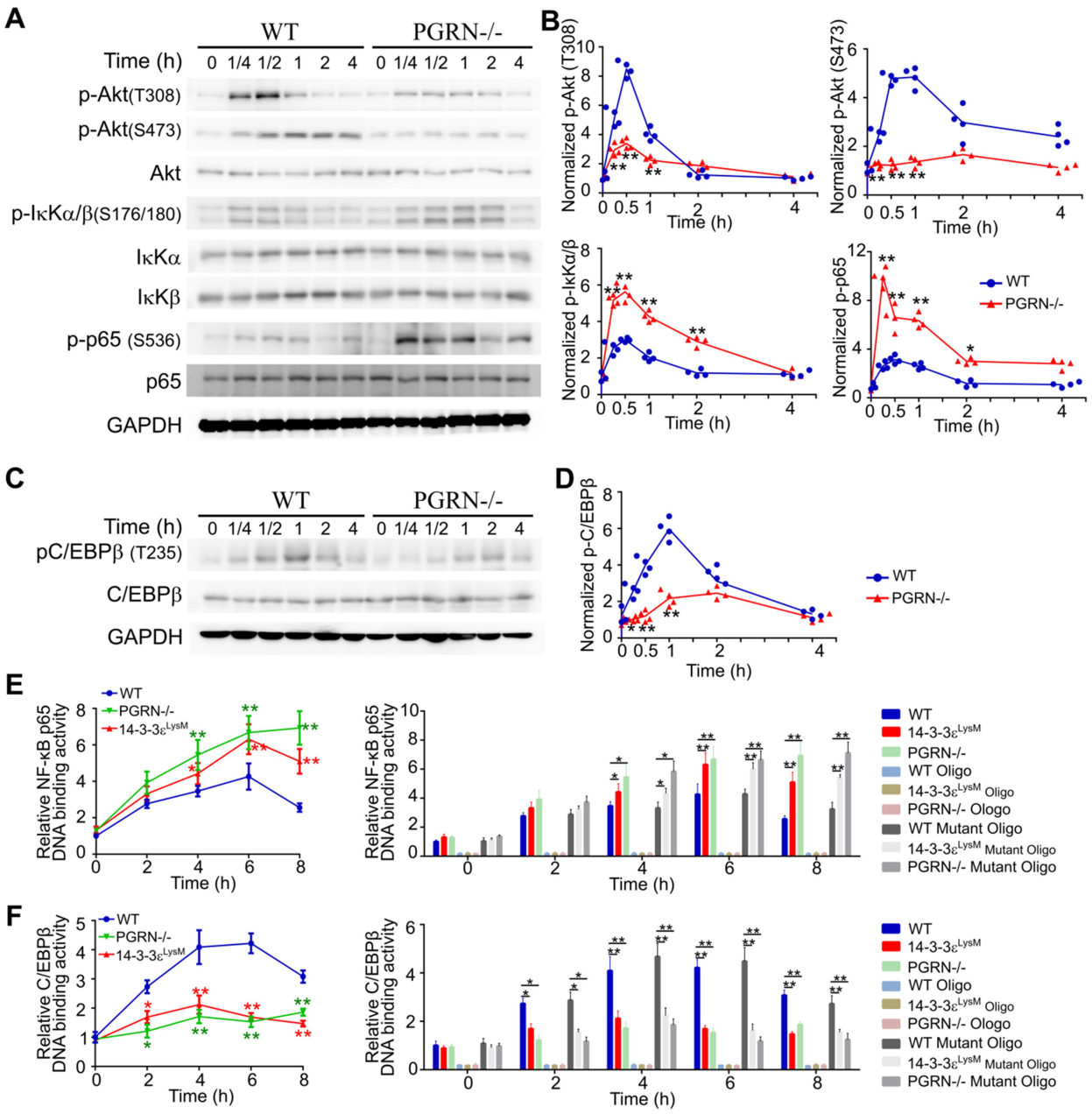

Supplementary Figure 23. PGRN signals through NF-κB and C/EBPβ during macrophage polarization. (A) Immunoblot analysis of selected signaling molecules in LPS stimulated WT and PGRN-/- macrophages. (B) Densitometry analysis of immunoblotting results shown in (A). (C) Immunoblot analysis of selected signaling molecules in IL-4 stimulated WT and PGRN-/- macrophages. (D) Densitometry analysis of immunoblotting results shown in (C). (E, F) NF-kB (E) and C/EBPβ (F) DNA binding activity in LPS and IL-4 stimulated WT, PGRN-/- and 14-3-3ε^{LysM} macrophages. For competitive binding studies, functional (oligo) or nonfunctional (mutant oligo) oligonucleotides were used according to the manufacturer's instructions. Data are mean ± SD; n = 4 biological replicates; * $P < 0.05$; * * $P < 0.01$. Significant difference was analyzed by unpaired Student's t-test (B, D) or one-way ANOVA with post hoc Bonferroni test (E, F).

Supplementary text for Tables

Table 1. Gene expression analysis of 14-3-3ε^{LysM} versus 14-3-3ε$^{f/f}$ BMDMs stimulated with LPS. Differential gene expression comparison between 14-3-3ε^{LysM} and 14-3-3ε$^{f/f}$ BMDMs (n=3 biological replicates) using DEseq2. Comparisons of gene expression between biological groups for which the adjusted p-values were <0.05 were considered significant. Top 100 up- or down-regulated genes in 14-3-3ε^{LysM} BMDMs compared to 14-3-3ε$^{f/f}$ were shown in the table.

Table 2. Gene expression analysis of 14-3-3ε^{LysM} versus 14-3-3ε$^{f/f}$ BMDMs stimulated with IL-4. Differential gene expression comparison between 14-3-3ε^{LysM} and 14-3-3ε$^{f/f}$ BMDMs (n=3 biological replicates) using DEseq2. Comparisons of gene expression between biological groups for which the adjusted p-values were <0.05 were considered significant. Top 100 up- or down-regulated genes in 14-3-3ε^{LysM} BMDMs compared to 14-3-3εf/f were shown in the table.